Molecular Therapy
Oncolytics
Original Article

AMERICAN SOCIETY of GENE & CELL THERAPY

# A PD-L1-Based Cancer Vaccine Elicits Antitumor Immunity in a Mouse Melanoma Model

Zhibing Lin,[1,2] Yan Zhang,[1,2] Huaman Cai,[1,2] Fuqiang Zhou,[1,2] Hongjun Gao,[3] Li Deng,[4] and Rongxiu Li[1,2,3]

[1]State Key Laboratory of Microbial Metabolism and School of Life Sciences and Biotechnology, Shanghai Jiao Tong University, 800 Dong Chuan Road, Shanghai 200240, China; [2]Engineering Research Center of Cell and Therapeutic Antibody, Ministry of Education, Shanghai Jiao Tong University, Shanghai, China; [3]Ruikang Hospital Affiliated with Guangxi University of Chinese Medicine, Shanghai, China; [4]Shanghai HyCharm, Inc., Shanghai, China

**Engagement of programmed death 1 receptor (PD-1) and its ligand PD-L1/2 induces a signal transduction pathway that inhibits the activity of tumor-infiltrating cytotoxic T lymphocytes and promotes tumor growth and metastasis. Antibodies blocking PD-1 or PD-L1 can restore antitumor T cell responses and cause long-term remission in a subset of cancer patients with advanced or refractory tumors. In this study, we asked whether PD-L1 vaccination could confer tumor control in mouse tumor models. To address the central tolerance toward self-molecules, we fused the extracellular domain of PD-L1 (PD-L1E) to the C-terminal of the translocation domain of diphtheria toxin (DTT). DTT is able to elicit CD4+ T cell responses required for inducing robust immune responses against self-molecules. The fusion molecule is called DPDL1E. When formulated with incomplete Freund's adjuvant (IFA), DPDL1E elicited robust immune responses biased toward the Th1 type and inhibited tumor growth in both preventive and therapeutic mouse tumor models. We further showed that the anti-DPDL1E sera blocked PD-L1 binding to PD-1 *in vitro*. The DPDL1E vaccination increased the levels of tumor-infiltrating T lymphocytes (TILs) and reduced the levels of myeloid-derived suppressor cells (MDSCs) as well as exhausted LAG3+PD-1+ CD8+ T cells. All of these data suggest that DPDL1E vaccination reverses the suppressive phenotype of the tumor microenvironment and that it is a promising strategy for cancer therapy.**

## INTRODUCTION

As one of the immune checkpoint inhibitors, PD-1 and its ligands PD-L1 and PD-L2 mediate a signaling pathway critical for maintenance of peripheral tolerance.[1] PD-1 is highly expressed on the surface of activated immune cells, including T cells, B cells, natural killer T cells, macrophages, and dendritic cells. PD-L1 is also expressed on activated immune cells such as T cells, B cells, macrophages, and dendritic cells. In addition, the expression of PD-L1 on the surface of many tissue cells, including those of the heart, lung, thymus, spleen, and kidney, is upregulated after interferon γ (INF-γ) stimulation. In contrast, the expression of PD-L2 is restricted to dendritic cells, macrophages, mast cells, and a subset of B cells.[1,2] The PD-1/PD-L1 pathway inhibits T cell antigen receptor signaling (thereby blocking cytokine production), inhibits T cell proliferation and differentiation, and promotes apoptosis of effector T cells as well as development of regulatory T (Treg) cells.[3,4]

The PD-1/PD-L1 pathway plays a dominant role in tumor immune evasion. PD-L1 is overexpressed in a variety of cancer types and tumor-associated antigen-presenting cells.[5–8] Overexpression of PD-L1 in the tumor microenvironment and peripheral blood is associated with a poor prognosis for cancer patients.[5,9–11] When PD-1 on activated T cells interacts with PD-L1 on tumor cells, tumor cells are protected from cytotoxic lysis, whereas T cells are functionally impaired and lapse into anergy, exhaustion, or apoptosis.[12–15] Monoclonal antibodies (mAbs) targeting PD-L1 or PD-1 have been approved for clinical treatment of several cancer types, particularly advanced solid tumors.[15–17]

However, therapeutic mAbs have their limits for clinical application because of the requirement of frequent administration and high cost. In this study, we tried to address these issues by taking an active immunization approach. We designed a vaccine targeting PD-L1 and assessed its immunogenicity and anti-tumor efficacy in mice. Our data showed that the PD-L1 vaccine reversed the suppressive functions of the PD-1/PD-L1 pathway in the tumor microenvironment and provided tumor control in both preventive and therapeutic mouse melanoma models. Therefore, the PD-L1 vaccine is promising as an alternative strategy for anti-PD-L1 mAb-based cancer therapy.

## RESULTS

### The Design and Purification of the DPDL1E Antigen

The tertiary structure of PD-L1 is composed of an extracellular domain (ECD), a transmembrane domain, and an intracellular region.[18,19] Because the ECD is responsible for binding of PD-1, we have chosen this domain as an immunogen. Because of central tolerance, the ECD is not immunogenic by itself. To break immune self-tolerance, we fused the ECD to the C-terminal of a carrier protein, diphtheria toxin (DTT) (Figure 1A and 1B).[20,21] The fusion molecule is designated DPDL1E. The protein was expressed in *E. coli* with a glutathione S-transferase (GST) fusion tag and purified by GST affinity chromatography. After removing the GST tag with

Received 7 December 2018; accepted 14 June 2019;
https://doi.org/10.1016/j.omto.2019.06.002.

**Correspondence:** Rongxiu Li, State Key Laboratory of Microbial Metabolism and School of Life Sciences and Biotechnology, Shanghai Jiao Tong University, 800 Dong Chuan Road, Shanghai 200240, China.
**E-mail:** rxli@sjtu.edu.cn

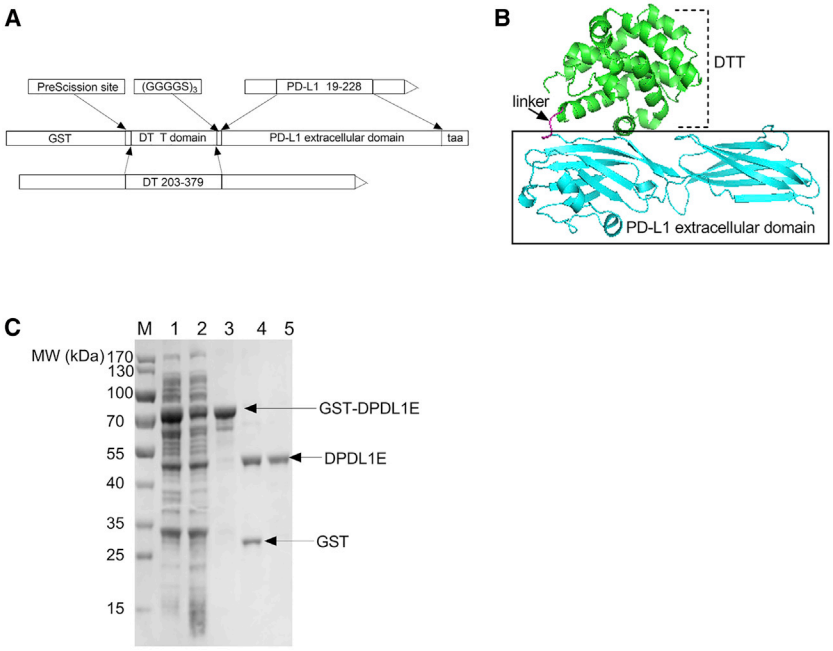


**Figure 1. Design of the DPDL1E Vaccine Antigen and Its Recombinant Preparation**

(A) Schematic representation of the DPDL1E antigen linear structure. (B) Structure model of DPDL1E. (C) SDS-PAGE analysis of DPDL1E antigen expression and purification. Lane 1: induced whole-cell lysate of DPDL1E with the GST tag. Lane 2: induced supernatant of DPDL1E with the GST tag. Lane 3: purified recombinant protein of DPDL1E with the GST tag. Lane 4: product mixture of GST-DPDL1E after PSP digestion. Lane 5: purified DPDL1E.

PreScission protease (PSP), the molecular weight of the protein was 43.5 kDa (Figure 1C). The protein was further purified to reduce the level of endotoxin contamination to less than 0.1 endotoxin units (EU)/mL.

### DPDL1E Immunization Induced PD-L1-Specific Humoral Immune Responses

To examine the immunogenicity of DPDL1E, we first measured the antibody responses by ELISA with the sera of both C57BL/6 and BALB/c mice immunized with either DPDL1E or DTT. Indeed, anti-PD-L1 antibodies were induced in all DPDL1E mice, whereas no PD-L1-specific antibodies were found in DTT-immunized mice (Figure 2A). Furthermore, we found that the immunoglobulin G (IgG) subclasses were composed of IgG1, IgG2a, IgG2b, and IgG3 (Figure 2B) and that the level of IgG2 was higher than those of IgG1 and IgG3, indicating that the immune responses were biased toward the Th1 type. The DTT-specific IgG1 was higher than the other antibody subclasses in DPDL1E-immunized mice (Figure 2B), indicating that anti-DTT immune responses were biased toward the Th2 type. To test the function of anti-PD-L1 antibodies, we performed a binding assay *in vitro* and found that the DPDL1E antisera could efficiently block PD-L1 and PD-1 interaction (Figure 2C) and that the degree of inhibition was correlated with the antibody titers (Figure 2D). In a parallel experiment, we used a PD-L1 mAb (10F.9G2) in *in vitro* binding assays. We found that the antibody concentration required to achieve the same level of inhibition was 11.25 μg/mL (Figure 2E).

### DPDL1E Vaccine-Induced Cytotoxic T Lymphocyte (CTL) Response

Because the vaccine induced a Th1-biased type of immunity, we examined the PD-L1-specific CTL response using a lactate dehydrogenase (LDH) release assay. Lymphocytes from DPDL1E-immunized mice were used as effector cells, and PD-L1+ B16-F10 cells were used as target cells. As expected, a significantly high level of cytotoxic activity was observed in DPDL1E-immunized mice compared with DTT-immunized mice ($p < 0.01$) (Figure 3A). Moreover, splenocytes from DPDL1E-immunized mice had a higher stimulation index than those from DTT-immunized mice with His-PD-L1 as a stimulator *in vitro* ($p < 0.05$), indicating that PD-L1-specific memory T cells had developed (Figure 3B). We measured the cytokine levels in the culture supernatants by ELISA. Compared with the DTT control group, the concentrations of interleukin-2 (IL-2), IFN-γ, and tumor necrosis factor alpha (TNF-α) were increased (153.25 pg/mL versus 975.25 pg/mL, 147.5 pg/mL versus 936.25 pg/mL, and 26.32 pg/mL versus 111.25 pg/mL, respectively). We further analyzed PD-L1-induced T cell proliferation *in vitro* by carboxyfluorescein succinimidyl ester (CFSE) profiling (Figure 3C) and found that PD-L1-specific CD8+ T cells and CD4+ T cells were present in immunized mice splenocytes (Figure 3D), demonstrating that DPDL1E vaccination can elicit PD-L1-specific cellular immune responses.

### DPDL1E Inhibits Tumor Growth in a Preventive Mouse Model

To evaluate the efficacy of the vaccine in tumor growth control, we challenged DPDL1E-immunized mice with B16-F10 cells (Figure 4A) and monitored tumor development in comparison with DTT- or PBS-treated mice. We found that the DPDL1E vaccination significantly inhibited tumor growth, and the median survival was increased from 16 days (PBS group) and 15 days (DTT group) to 23 days (DPDL1E group). Notably, 25% of DPDL1E-vaccinated mice had no tumor growth, and their survival was prolonged beyond 60 days (Figures 4B, 4C, and S1A). We also noted that the tumor volumes of DPDL1E-immunized mice on day 19 after tumor challenge were correlated with the PD-L1-specific antibodies titers on day 7 after the third immunization ($R^2 = 0.6425$) (Figure 4D), which indicated that anti-PD-L1 antibodies are the major contributors to tumor control. In parallel experiments, we found that the DPDL1E vaccine also inhibits tumor growth in the CT26 colon cancer mouse model (Figure S2).

Because B16-F10 is a metastatic cell line, we asked whether DPDL1E vaccination could inhibit metastasis to the lungs. We applied the

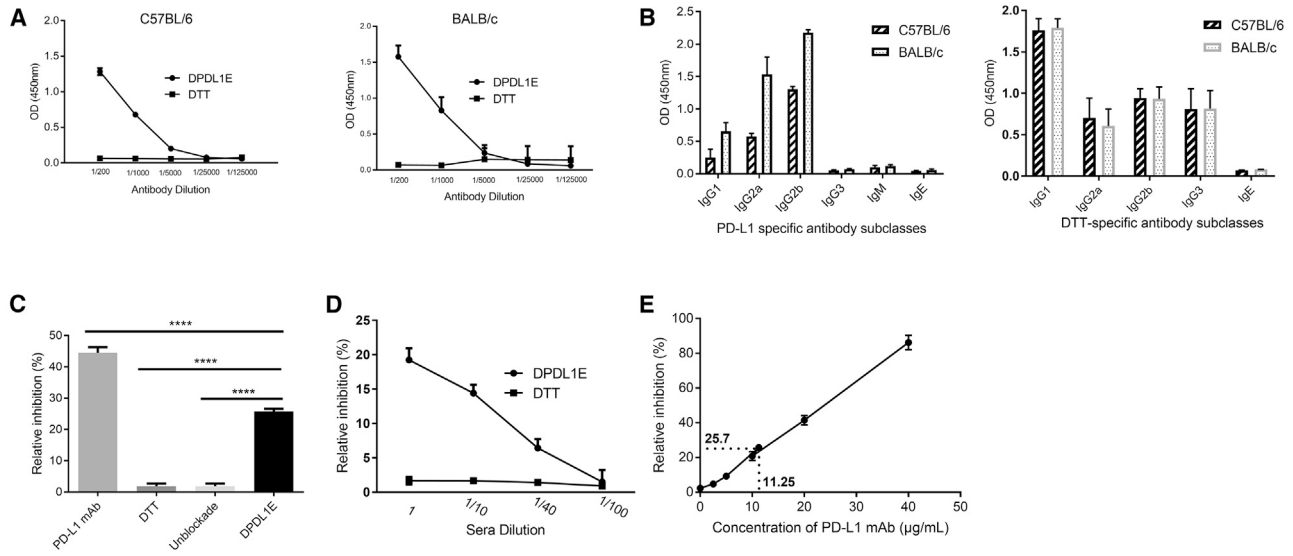


**Figure 2. Antibody Responses Induced by DPDL1E Vaccination in C57BL/6 and BALB/c Mice**

(A) Mice (n = 8) were immunized with DPDL1E three times at 2-week intervals. One week after the third immunization, the antibody titers were measured by ELISA using His-tagged PDL1 recombinant protein as a coating antigen. DTT-immunized serum was used as a negative control. (B) The levels of PD-L1- and DTT-specific antibody subclasses induced by DPDL1E vaccination. Sera were isolated from C57BL/6 and BALB/C mice immunized with the DPDL1E vaccine. The levels of the indicated antibody subclasses were measured by ELISA. (C) The sera from DPDL1E-immunized mice inhibited binding of PD-L1 to PD-1. PD-L1 mAb at 20 μg/mL was used as a positive control, and sera from DTT-immunized mice and PBS were used as a negative control and blank control, respectively. (D) The inhibition efficiency of sera at different concentrations was tested and compared with the control group. (E) A standard curve was created (relative inhibition versus concentration of PD-L1 mAb) to calculate the effective anti-PD-L1 concentration *in vitro*. ****$p < 0.0001$.

B16-F10 metastatic model. The mice were sacrificed on day 14 thereafter, and the lungs were checked for tumor nodules (Figure 4E). An average of 257 and 242 nodules were found in the PBS and DTT groups, respectively, whereas an average of 92 and 79 nodules were found in the DPDL1E group and mAb group, respectively. Furthermore, the number of large nodules (more than 3 mm in diameter) were significantly lower in the DPDL1E group of mice. In a parallel experiments using mAb, we found no significant difference between the DPDL1E group and mAb group in terms of the total number of nodules and the numbers of large nodules (Figure 4F-G), indicating that DPDL1E vaccination achieved a similar level of protection as mAbs.

### DPDL1E Inhibits Tumor Growth in a Therapeutic Mouse Melanoma Model

To evaluate the therapeutic efficacy of the DPDL1E vaccine, B16-F10 tumor-bearing C57BL/6 mice were established as described previously.[22,23] When the tumors were palpable, the mice were treated with DPDL1E or the DTT vaccine. For comparison, another group of mice was treated with a mAb (Figure 5A). Compared with the isotype or DTT control groups, both the DPDL1E vaccine and PD-L1 mAb inhibited tumor growth (Figure 5B). The mean survival time of each group was 16.25 days (DTT group), 16.25 days (isotype group), 19 days (DPDL1E group), and 20.25 days (PD-L1 mAb group) (Figure 5C). More strikingly, tumor growth was markedly inhibited in a subset of mice in both the DPDL1E vaccine- and PD-L1 mAb-treated groups (Figure S1B).

To verify that anti-PD-L1 antibodies were the major contributors, we purified antibodies from the immunized mice and transferred them into unimmunized tumor-bearing mice (Figure 5D). Compared with antibodies from the control groups, antibodies from DPDL1E immunized mice inhibited tumor growth (Figure 5E) and prolonged survival (Figure 5F). These data suggest that PD-L1-specific antibodies play a key role in tumor control.

To test whether a combination of DPDL1E and PD-L1 mAb could benefit therapy, we immunized tumor-bearing mice following the schedule in Figure 5A. Combination of the DPDL1E vaccine and PD-L1 mAb synergistically inhibited tumor growth (Figure 5G) and prolonged the survival time (Figure 5H). These data indicate that the anti-PD-L1 by vaccine approach is promising as an alternative or combinatorial cancer therapy.

### DPDL1E Vaccination Increases the Ratio of CD8+ T Cells/Myeloid-Derived Suppressor Cells (MDSCs) in Tumors and Peripheral Blood

Because the level of tumor-infiltrating lymphocytes (TILs) and the ratio of CD8+ T cells/MDSCs have been shown to be associated with anti-tumor immunity,[22,23] we measured the level of CD8+ T cells in the B16-F10 melanoma model using an immunohistochemistry (IHC) assay. Compared with the DTT-treated group, DPDL1E vaccination increased the level of CD8+ T cell infiltration in both preventive (Figures 6A and S3A) and therapeutic mouse melanoma models (Figures 6B and S3B). In the therapeutic setting, the levels

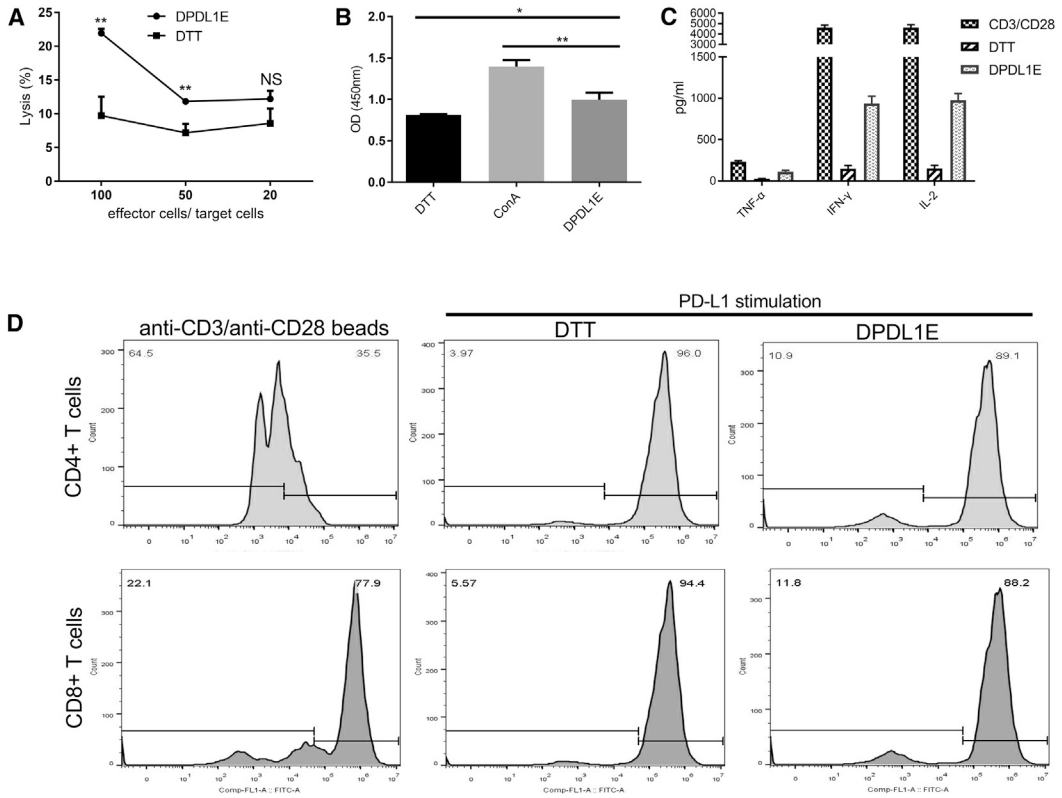


**Figure 3. The CTL Response Induced by DPDL1E Vaccination**

(A) Lymphocytes from spleens of DPDL1E- and DTT-immunized mice were used as effector cells. PD-L1-positive expressed B16-F10 cells were used as target cells. Cytotoxicity was assessed with an LDH release assay. Statistically significant differences were determined using Student's t test. (B) Lymphocytes isolated from DTT- and DPDL1E-immunized mice were stimulated with His-PD-L1 recombinant protein or Con A for 72 h. Cell proliferation was measured with the CCK-8 method. (C) The concentrations of TNF-α, IFN-γ, and IL-2 in supernatant after 72 h stimulation. The cytokines were detected using an ELISA kit. Anti-CD3/CD28 beads (0.5 μg/mL) were used as a positive control. (D) Proliferation of T cells was determined using a CFSE-based assay *in vitro*. CD8+ and CD4+ T cells were gated and analyzed using FCM. Both CD8+ and CD4+ T cells proliferated more than the DTT control group after His-PD-L1 stimulation. Statistically significant differences were calculated by Student's t test. NS, not significant; *$p < 0.05$; **$p < 0.01$.

of CD8+ T cells in DPDL1E-vaccinated mice were 5 times higher than in control mice (Figure 6B). In a parallel experiment using the anti-PD-L1 mAb, the level of CD8+ T cell infiltration was also significantly increased compared with the isotype control (Figure 6B). The flow cytometry (FCM) data further confirmed that the DPDL1E vaccine significantly increased T cell infiltration into tumors (Figure 6C).

Next we examined the ratio of CD8+ T cells/MDSCs in tumor tissues and peripheral blood using an FCM assay. The data showed that DPDL1E increased the levels of CD8+ T cells (Figure 6D) and decreased the levels of MDSCs in tumors (Figure 6E). The ratio of CD8+ T cells/MDSCs was higher in the DPDL1E and PD-L1 mAb groups than in the isotype or DTT control groups (Figure 6F). In addition, the DPDL1E vaccine increased the level of CD8+ T cells (Figure 7A) and decreased the level of MDSCs in peripheral blood (Figure 7B). Therefore, the ratio of CD8+ T cells/MDSCs in peripheral blood was increased by the vaccine (Figure 7C). These data suggest that the DPDL1E vaccine reverses the suppressive tumor microenvironment to permit immune-mediated tumor rejection.

### The DPDL1E Vaccine Upregulated the Level of PD-L1 and Decreased the Level of LAG3+ PD-1+ T cells in Tumors

Increased expression of PD-1 and LAG3 on TILs is an indicator of impaired T cell function.[24] To examine whether the DPDL1E vaccination has any effect on the expression of PD-1 and LAG3 on TILs, we analyzed their levels in DPDL1E-treated mice as well as in DTT-, isotype-, and PD-L1 mAb-treated mice by FCM. The gating strategies for frequency analyses are shown in Figure S4. The levels of PD-L1+ cells in CD45+ cells from DPDL1E-treated mice were higher than those from DTT- and isotype-treated mice (Figure 8A), whereas the levels in PD-1+ CD45+ cells from DPDL1E-treated mice were lower than in those from DTT- and isotype-treated mice (Figure 8B). The levels of LAG3+ as well as PD-1+ LAG3+ CD8+ T cells from DPDL1E- or PD-L1 mAb-treated mice were lower than those from DTT- and isotype–treated mice (Figures 8C and 8D). There was no significant difference between DPDL1E-treated mice and PD-L1 mAb-treated mice regarding the levels of LAG3+ T cells or

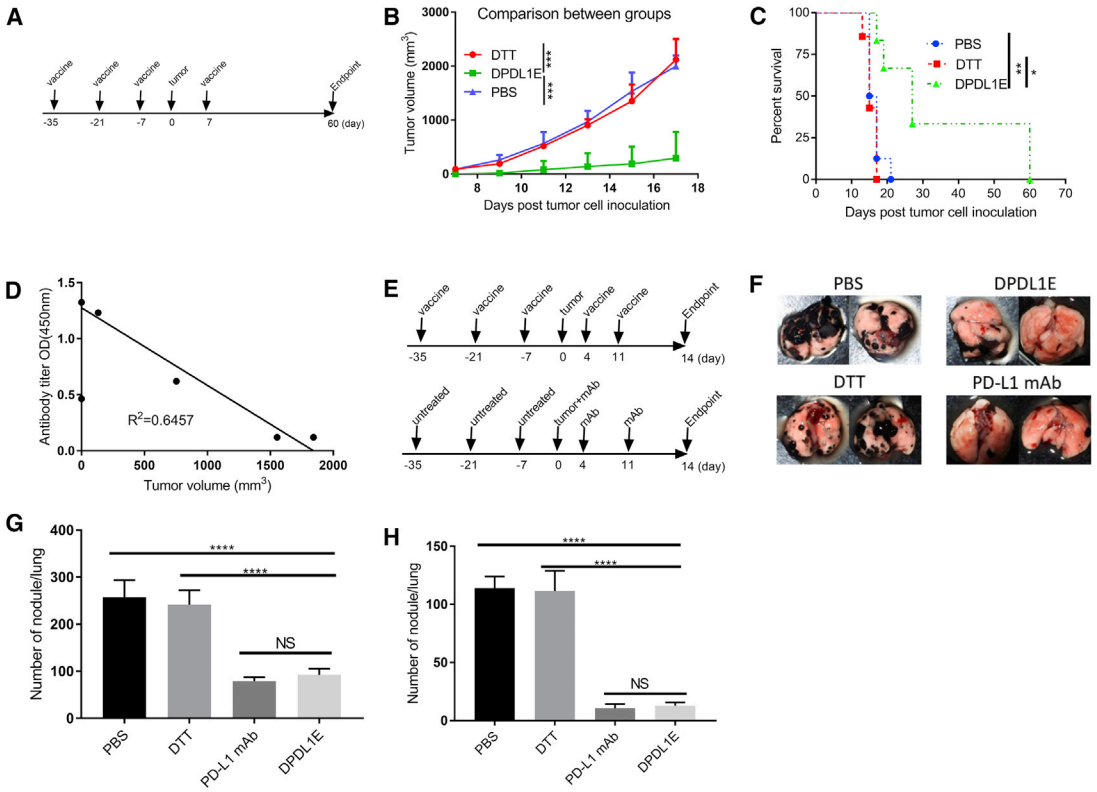


**Figure 4. Tumor Growth Was Inhibited in DPDL1E-Vaccinated Mice**

(A) Experimental workflow of the mouse preventive model. Mice were immunized subcutaneously three times at 14-day intervals. On day 7 after the third immunization, mice were injected s.c. with tumor cells. On day 7 after tumor challenge, the fourth immunization was administered. (B) Tumor volume measurements were performed to evaluate tumor growth. The endpoint was predefined by mouse death or a tumor reaching 2 cm in any direction. Statistically significant differences were determined by Mann-Whitney *U* test. (C) A mouse survival curve was constructed after the tumor challenge. Statistically significant differences were determined using a log rank test. (D) A scatterplot with tumor volumes on day 17 as the coordinates of the horizontal axis and serum antibody titers on day 7 after the third immunization as the coordinates of the vertical axis. The correlation coefficient was determined using GraphPad Prism 6 software. (E) The schedule for the metastatic mouse model. (F) Representative images of lung metastasis. (G and H) The total number of nodules (G) and the number of large nodules (H) in the lung. *$p < 0.05$, **$p < 0.01$, ***$p < 0.001$, ****$p < 0.0001$.

PD-1+ LAG3+ T cells. These data suggested that the DPDL1E vaccine decreased inhibitory receptor expression in the tumor microenvironment.

### No Adverse Tissue Damage Was Found in DPDL1E-Vaccinated Mice

To examine the safety of the DPDL1E vaccine *in vivo*, we performed histological analyses of tissues from different treatment groups on day 90 after the third immunization. There was no apparent damage detected by H&E staining (Figure S5A). We further analyzed blood cell counts using an automatic hematology analyzer. The levels of red blood cells (Figure S5B), white blood cells (Figure S5C), or platelets (Figure S5D) were not significantly different between DPDL1E-immunized mice and DTT- or PBS-treated mice. In addition, the mouse body weights were similar among all experimental groups (Figure S5E). These data suggest that DPDL1E vaccination is a safe and tolerable approach for cancer therapy.

## DISCUSSION

In this study, we found that immunization of mice with a designed recombinant DPDL1E vaccine delayed tumor growth and increased survival time. The antibodies induced by the DPDL1E vaccine blocked PD-L1 binding to PD-1 *in vitro* and conferred tumor growth control in an adoptive transfer model. Our analyses revealed that the blocking ability of antibodies was significantly associated with antibody titer. We also found that, compared with control groups, the DPDL1E vaccine increased CD8+ T cell infiltration and decreased T cell anergy-associated receptor PD-1 and LAG3 expression in a mouse tumor model.

We determined that the DPDL1E vaccine can induce PD-L1-specific-T cells. Ahmad et al.[25] and Munir et al.[26] have shown that PD-L1-specific CTL enhances antileukemic immunity and can directly lyse PD-L1+ leukemia cells. Thus, a vaccine targeting PD-L1 may have added benefits for cancer therapy. Because therapeutic mAbs restored anti-tumor immunity only in a subset of

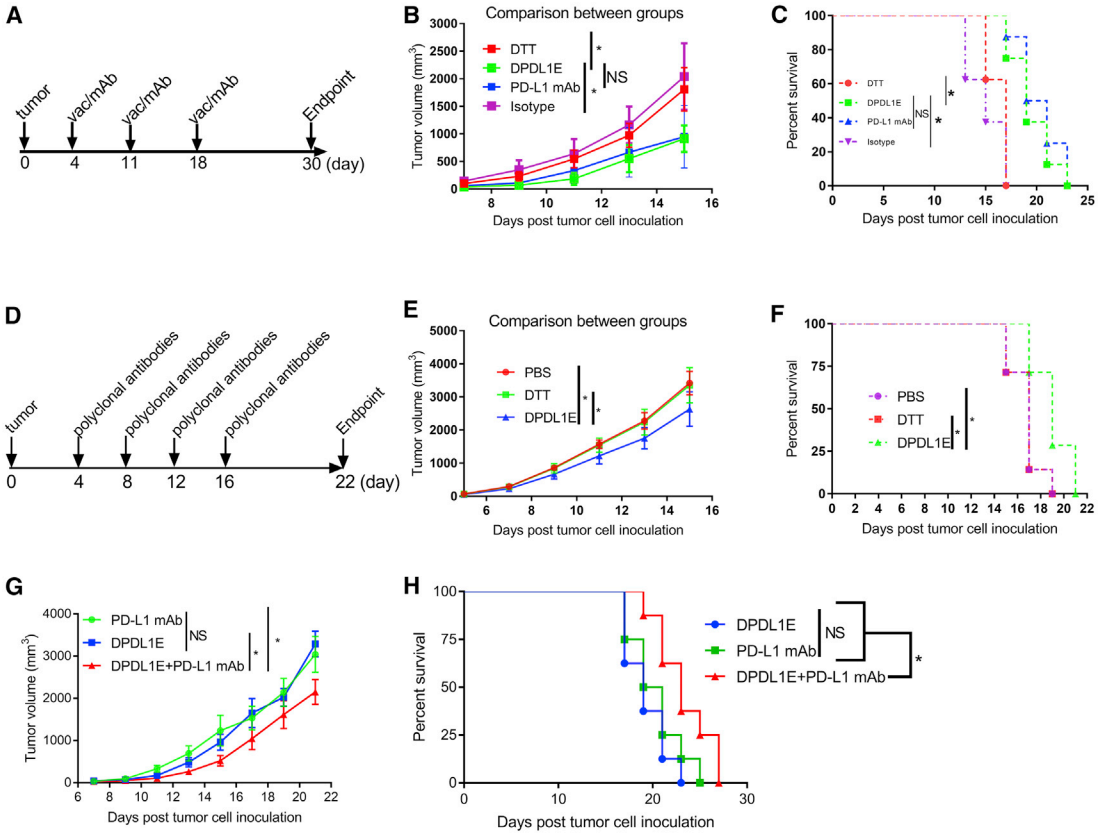


**Figure 5. Therapeutic Efficacy of the DPDL1E Vaccine and Purified Polyclonal Antibody**

(A) The vaccination (vac) and mAb treatment schedule for the therapeutic mouse melanoma model. (B) Tumor growth curves of different treatment groups after the schedule in (A). C57BL/6 mice (n = 8) were challenged with $2 \times 10^5$ B16-F10 cells. On day 4 after the challenge, DPDL1E vaccine was administered s.c. In parallel experiments, PD-L1 mAb were administered i.p. Mann-Whitney *U* test was used to evaluate statistically significant differences. (C) The survival rates of different treatment groups after the schedule in (A). Statistically significant differences were determined using log rank test. (D) The purified polyclonal antibody treatment schedule for the therapeutic mouse melanoma model. (E) Tumor growth curves of different treatment groups after the schedule in (D). C57BL/6 mice (n = 8) were challenged with $2 \times 10^5$ B16-F10 cells. On day 4 after the challenge, purified polyclonal antibody from the DPDL1E-immunized group or the control groups were administered i.p. Mann-Whitney *U* test was used to evaluate statistically significant differences. (F) The survival rates of different treatment groups after the schedule in (D). (G and H) Tumor growth curves (G) and survival rates (H) of different treatment groups. Statistically significant differences were determined using log rank test. *$p < 0.05$.

cancer patients, the PD-L1 vaccine may increase the rate of response by virtue of a PD-L1-specific T cell response. The limitation of this study is that we have not identified PD-L1 T cell epitopes to evaluate a contribution of the T cell response alone in tumor control. However, PD-L1-specific CD8+ T cell and CD4+ T cells were detected *in vitro*.

MDSCs are the major immune suppression cells in both peripheral blood and the tumor environment.[27] MDSCs levels in cancer patients are correlated with clinical stage, and higher MDSCs levels in peripheral blood are associated with a poorer prognosis.[28] We showed that the DPDL1E vaccine confers tumor growth control in part via down-regulation of MDSC levels in both peripheral blood and the tumor microenvironment. The levels of PD-1+ and LAG3+ T cells are indicators of T cell dysfunction.[29,30] The DPDL1E vaccine not only increased T cell infiltration into tumors but also decreased the expression of PD-1 and LAG3 on T cells. These data indicate that the DPDL1E vaccine reverses immune suppression in the tumor microenvironment.

Dendritic cells (DCs) and macrophages play an important role in tumor control and progression.[31,32] Immune profiling of B16 F10 tumors has identified tumor-infiltrating DCs and macrophages.[33] Antibodies targeting PD-L1 or PD1 enhance DC-mediated T cell activation[34,35] and shift macrophage polarization toward the M1 type.[36] It warrants further study whether DCs and macrophages in the tumor microenvironment contribute to tumor growth control by the DPDL1E vaccine.

Because many immune cell types express PD-L1,[37] one safety concern regarding the PD-L1 vaccine is be off-target toxic effects. Our results indicate that, in a period of 60 days, these effects are not evident in

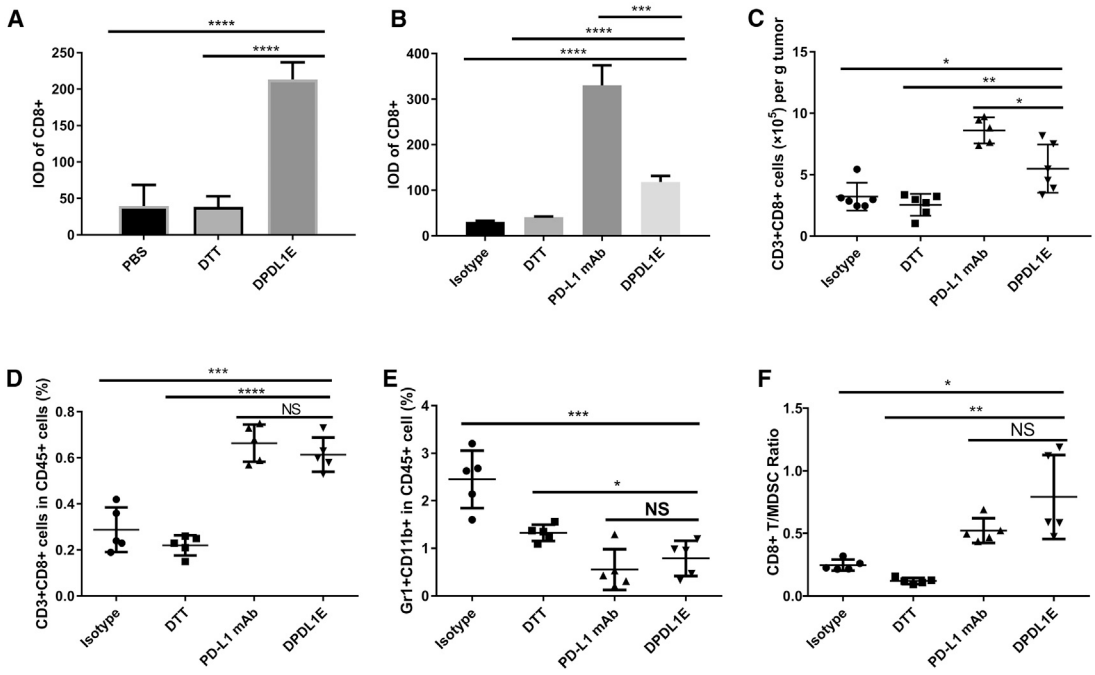


**Figure 6. The DPDL1E Vaccine Increased the Levels of TILs and the Ratio of CD8+ T Cells/MDSCs in Tumor Tissues**

(A and B) Tumor tissues isolated from mice of preventive groups (A) and therapeutic groups (B) were stained with anti-CD8α monoclonal antibody. The IOD was determined by Image-Pro Plus 4.5 software. (C) TILs were further confirmed using FCM. (D)The ratio of CD3+ CD8+ T cells in CD45+ was analyzed using FCM. (E) The ratio of MDSCs in CD45+ was also analyzed using FCM. (F) The ratio of CD8+ T cells/MDSCs was calculated and analyzed. Student's t test was used to determine statistically significant differences. *$p < 0.05$, **$p < 0.01$, ***$p < 0.001$, ****$p < 0.0001$.

DPDL1E-immunized mice. A longer term of safety monitoring is warranted for future vaccine development.[38,39]

According to the data, the major effect of DPDL1E therapy is shown in the preventive model. There are two aspects that should be seriously considered in tumor vaccine evaluation. Compared with mAbs or chemotherapy, the vaccine needs time to trigger the immune response and is more dependent on the status of the immune system. In the present B16-F10 mouse therapy model, tumor progression is so quick that the immune system does not have enough time to control solid tumor growth. The increased volume of tumors does not only weaken the immune response but also promotes the formation of a tumor-suppressive microenvironment. The vaccine strategy would be more effective for residue tumors and early stages of tumors. According to clinical data, people with early cancer have a good prognosis and long survival time.[40,41] Our results indicate that preexisting PD-L1-specific antibodies can help control tumor growth. The vaccine targeting PD-L1 can been used for these patients after surgery for persistent tumor control. Compared with mAbs, vaccines targeting PD-L1 can reduce the economic burden patients, especially people in less developed countries.

We conclude that the DPDL1E vaccine targeting PD-L1 induced a PD-L1-specific immune response and delayed tumor growth *in vivo*. These results indicate a promising avenue for future research in the quest for cancer vaccine design. The heterogeneity and diversity of tumors indicate that tumor cells have different morphological and phenotypic profiles.[42] The complex nature of cancer is why single therapy has limited efficacy.[43] Thus, combination therapy is necessary to combat advanced stages of cancers. Checkpoint blockade cooperates with a cancer vaccine to enhance antitumor immunity.[23,44] The combination of PD-L1/PD1 blockade and an oncolytic virus has been discussed in several studies.[45,46] Blockade of PD-L1/PD1 promotes the efficacy of chimeric antigen receptor T cell (CAR-T) adoptive therapy.[47,48] The DPDL1E vaccine combined with CAR-T or an oncolytic virus may yield better performance in cancer therapy. Vaccines targeting checkpoints should be considered and combined with other cancer therapy methods.

## MATERIALS AND METHODS

### Cells and Mice

The murine B16-F10 melanoma cell line and the CT26 colon carcinoma cell line were purchased from the ATCC and cultured in DMEM (Thermo Fisher Scientific, San Jose, CA, USA) supplemented with 10% fetal calf serum (FCS), 100 units/mL penicillin, and 100 μg/mL streptomycin (Gibco, Grand Island, NY, USA). Female C57BL/6 and BALB/c mice were purchased from Slac Laboratory Animal (Shanghai, China) and housed in the Shanghai Jiao Tong University Laboratory Animal Center under specific pathogen-free (SPF) conditions. The mouse experiments were carried out following

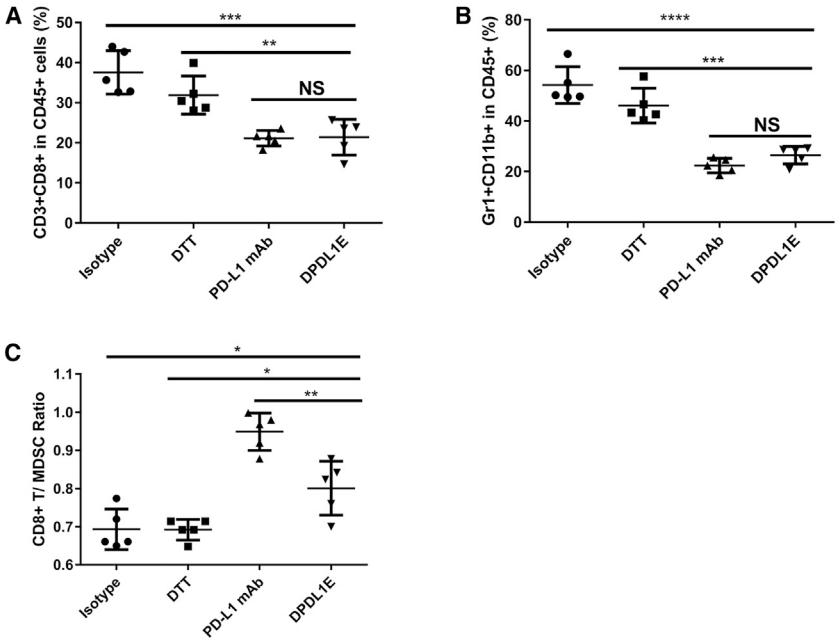


**Figure 7. The DPDL1E Vaccine Increased the Ratio of CD8+ T Cells/MDSCs in Peripheral Blood**

(A and B) The ratio of CD3+ CD8+ T cells (A) and the ratio of MDSCs (B) in CD45+ were analyzed using FCM. (C) The ratio of CD8+ T cells/MDSCs in peripheral blood was calculated and analyzed. *$p < 0.05$, **$p < 0.01$, ***$p < 0.001$, ****$p < 0.0001$. Student's t test was used to determine statistically significant differences.

protocols approved by the laboratory animal center of Shanghai Jiao Tong University.

### Gene Cloning and Vector Construction

The mouse PD-L1 gene (NM_021893.3) was amplified from total RNA of the C57BL/6 mouse spleen by RT-PCR using the PrimeScript RT Reagent Kit (Takara Bio, Tokyo, Japan), and the gene fragment was inserted into the PMD-18T vector (Takara Bio, Tokyo, Japan). Overlapping PCR was performed to generate the fusion gene DPDL1E consisting of DTT and the PD-L1 ECD (PDL1E). After *Eco*RI and *Xho*I digestion, the fusion gene fragment was inserted into the expression vector pGEX6p-1. All primers are listed in Tables S1 and S2.

### Protein Expression, Purification, and Analysis

DPDL1E and DTT were expressed as GST fusion proteins in *E. coli* BL21. The recombinant proteins were purified by GST affinity chromatography as described previously.[21] The GST tag was removed by PSP (GE Healthcare) treatment followed by GST affinity chromatography. Endotoxin was removed using Detoxi-Gel Endotoxin-Removing Columns (Thermo Scientific, USA). Endotoxin levels were monitored using a Limulus amebocyte lysate (LAL) test (GenScript, China). The DPDL1E protein was modeled using the *Ab Initio* Domain Assembly Server (AIDA) and visualized in Discovery Studio Visualizer 3.5.[21,49]

### Immunization and Tumor Challenge

For the tumor-preventive model, 4- to 6-week-old female C57BL/6 or BALB/c mice (n = 8) were immunized subcutaneously three times with the DPDL1E vaccine or DTT protein at 14-day intervals. For each mouse, the vaccine formulation contained 50 μg antigen, 30 μg poly(I:C) (Tocris Bioscience, MO, USA) in 50 μL PBS and 50 μL incomplete Freund's adjuvant (IFA; InvivoGen, San Diego, CA, USA).The DPDL1E vaccine was injected subcutaneously (s.c.) into the right flank or the dorsal part of the mouse. On day 7 after the third immunization, the mouse was injected s.c. with $2 \times 10^5$ B16-F10 melanoma cells or $2 \times 10^5$ CT26 colon carcinoma cells in the left forelimbs. On day 7 after tumor challenge, the fourth immunization was administered.

To evaluate the effect of DPDL1E on tumor metastasis, we used a lung metastasis model with slight modifications, as reported previously.[50] Briefly, $10^5$ B16-F10 cells were injected intravenously (i.v.) into immunized or non-immunized mice (n = 8), and the mice were sacrificed on day 14 for analysis of lung invasion (Figure 4E). The total number of tumor nodules and the number of large nodules (>3 mm) were assessed.

For the tumor therapy model, 4- to 6-week-old female C57BL/6 mice (n = 8) were challenged with a s.c. injection of $2 \times 10^5$ B16-F10 melanoma cells in the left forelimbs. When the tumors were palpable (4 days later), mice were immunized s.c. with 50 μg DPDL1E vaccine or 50 μg DTT protein or intraperitoneally (i.p.) administered 200 μg anti-PD-L1 mAb (10F.9G2, Bio X Cell, Japan) or 200 μg control rat IgG (Bio X Cell, Japan) three times at 7-day intervals.[22,23] DPDL1E (50 μg) and PD-L1 mAb (200 μg) were combined in the therapy model as described above. Tumor diameters were measured every other day with Vernier calipers, and the tumor volumes were calculated using the following formula: volume = $(\text{width}^2 \times \text{length})/2$.[51] The mice had to be sacrificed at a maximal tumor diameter of 2 cm for ethical reasons and were recorded as dead.

### Purified Polyclonal Antibody Therapy Model

The sera isolated from DTT- or DPDL1E-immunized mice were purified using a serum antibody purification kit (Abcam, Cambridge, MA, USA) according to the manufacturer's instruction. When the tumors were palpable (~4 days later), mice were i.p. administered 400 μg purified antibodies from DPDL1E-immunized mice or 400 μg control purified antibodies from DTT-immunized mice, three times at 3-day intervals. The tumor volumes were measured as described above.

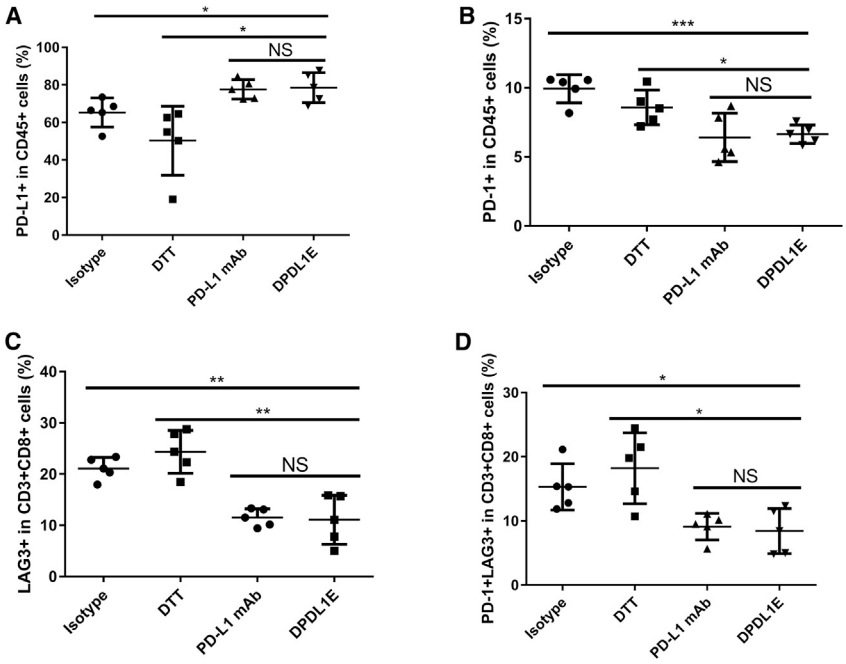


**Figure 8. The DPDL1E Vaccine Decreased the Ratio of PD-1+ Cells and Increased the Ratio of PD-L1+ Cells in Tumors**

(A) PD-L1+ cells were stained with anti-CD274-APC and anti-CD45-FITC. (B) PD-1+ cells were stained with anti-CD279-APC and anti-CD45-FITC. (C) LAG3+ cells were stained with anti-CD223-PE, anti-CD3-FITC, and anti-CD8-PerCP-Cy5.5. (D) LAG3+PD-1+ cells were stained with anti-CD279-APC, anti-CD223-PE, anti-CD3-FITC, and anti-CD8-PerCP-Cy5.5. All samples were detected using FCM, and the data were analyzed using FlowJo software. *$p < 0.05$, **$p < 0.01$, ***$p < 0.001$. Statistically significant differences were assessed using Student's t test.

### ELISA for Antibody Detection

Ninety-six-well plates (Corning Life Sciences, New York, USA) were coated with 100 μL of 1 μg/mL mouse PD-L1 recombinant protein (Sino Biological, Beijing, China) or DTT protein in sodium carbonate buffer (pH 9.6) overnight at 4°C. After washing with PBS and 0.05% Tween 20 (PBST), the plates were blocked with 3% BSA in PBST. The diluted mouse sera were added to wells and incubated for 1 h at 37°C. After washing, 100 μL of 1:5,000 diluted horseradish peroxidase (HRP)-labeled goat anti-mouse subclass antibodies (Thermo Fisher Scientific, San Jose, USA) were added to the wells, and the plates were incubated for 1 h at 37°C. Absorbance was determined at 450 nm using SpectraMax M5 (Molecular Devices, CA, USA).

### PD-L1 PD-1 Blockade Assay

Serum was isolated from DPDL1E- or DTT-immunized mice 7 days after the third immunization. 96-well plates (Corning Life Sciences, NY, USA) were coated with 100 μL of 5 μg/mL mouse PD-L1 recombinant protein (Acrobiosystems, Bethesda, MD, USA) overnight at 4°C. After washing, 100 μL serum from DPDL1E-immunized mice, 100 μL of 20 μg/mL PD-L1 mAb (10F.9G2, Bio X Cell, Japan), or 100 μL serum of DTT-immunized mice was added to the wells. The plates were incubated at room temperature for 1 h. After washing, 100 μL (2.5 μg/mL) biotin-labeled PD-1 protein (Acrobiosystems, Bethesda, MD, USA) was added to the wells and incubated for 1 h at 37°C. After washing, 100 μL HRP-labeled avidin was added to the wells and incubated for 1 h at 37°C. After washing, 200 μL 3,3',5 ,5'-tetramethylbenzidine (TMB) was added to the wells and incubated for 20 min at room temperature. After incubation, 50 μL 2 M $H_2SO_4$ was added to the wells, and absorbance was determined at 450 nm using SpectraMax M5 (Molecular Devices, Sunnyvale, CA, USA).

### Lymphocyte Proliferation Assay

C57BL/6 mice (n = 8) were immunized with the DPDL1E or DTT vaccine at 2-week intervals. One week after the third immunization, splenocytes were isolated for further study. Briefly, spleens were isolated from mice under sterile condition and ground into single cells. 5 mL red blood cell (RBC) lysis buffer (Sigma-Aldrich, USA) was added, followed by spinning for 5 min. The cells were filtered through a 70-μM filter (BD Lifesciences, USA) and counted. Splenocytes ($1 \times 10^6$ /mL in RPMI 1640 medium with 10% FCS) isolated from DPDL1E-immunized mice were cultured in 96-well plate (100 μL/well) and stimulated for 72 h with 50 μg/mL His-PD-L1, 5 μg/mL concanavalin A (Con A; Thermo Fisher Scientific, San Jose, CA, USA), or anti-CD3/CD28 beads (0.5 μg/mL). Splenocytes isolated from DTT-immunized mice were cultured in a 96-well plate and stimulated with 50 μg/mL His-PD-L1 as a negative control. Cell proliferation was measured using a Cell Counting Kit (CCK)-8 kit (Dojindo, Japan). After 72 h stimulation, the supernatant was collected for cytokine detection. The concentrations of TNF-α, IFN-γ, and IL-2 were measured using corresponding ELISA kits (Thermo Fisher Scientific, San Jose, CA, USA).

Splenocytes isolated from DPDL1E- or DTT-immunized mice were stained with CFSE (Dojindo, Japan) according to the manufacturer's instructions and cultured in RPMI 1640 medium containing 10% FCS and 20 units /mL IL-2. The cells were stimulated with His-PD-L1 protein (50 μg/mL) or anti-CD3/CD28 beads (0.5 μg/mL). After 72 h of stimulation, CD8+ and CD4+ T cell proliferation was analyzed by FCM after the cells were stained with anti-CD3-PE, anti-CD8-peridinin chlorophyll protein complex (PerCP)-Cy5.5, and anti-CD4-antigen-presenting cell (APC) (BD Lifesciences, USA).

### CTL Assay

PD-L1-positive expressed B16-F10 cells were used as target cells, as reported previously.[52] Lymphocytes isolated from DPDL1E-immunized mice were stimulated for 72 h with a His-PD-L1 protein and

used as effector cells. Effector cells and target cells were mixed at ratio of 100:1, 50:1, or 20:1 and incubated in Corning Life Sciences 96-well plates at 37°C for 4 h. CTL activities were detected using an LDH cytotoxicity detection kit (Biovision, USA).

### FCM Assay

A single-cell suspension of peripheral blood from tumor-bearing mice was stained with anti-CD3- fluorescein isothiocyanate (FITC), anti-CD8-PerCP-Cy5.5, anti-CD45-APC or anti-CD45-FITC, anti-CD11b-PerCP-Cy5.5, or anti-Gr1-phycoerythrin (PE). All FCM antibodies were purchased from BD Biosciences. Immune cells in tumor tissue were purified using tumor immune cell separation fluid (Tianjin Hao Yang, China) and stained with anti-CD3-FITC, anti-CD8-PerCP-Cy5.5, anti-CD45-APC or anti-CD45-FITC, anti-CD11b-PerCP-Cy5.5, or anti-Gr1-PE. Cells were also stained with anti-CD45-FITC, anti-CD274-APC (anti-PD-L1) or anti-CD3-FITC, anti-CD8-PerCP-Cy5.5, anti-CD279-APC (anti-PD-1), or anti-CD223-PE (anti-LAG3). Cells were analyzed by FCM (Beckman CytoFLEX, USA). Data were analyzed using FlowJo software (Tree Star, Ashland, OR, USA).

### Safety Evaluation

Different organs isolated from immunized mice were fixed in 4% phosphate-buffered formalin for 24 h and embedded in paraffin. The tissue sections were stained with H&E. The cellular composition of mouse blood was analyzed by an automatic hematology analyzer (Mindray, China). For immunohistochemical detection of CD8+ T cell infiltration, tumor tissue sections were stained with anti-CD8α (rabbit mAb, D4W2Z XP, Cell Signaling Technology, USA). The integral optical density (IOD) of tumor-infiltrating CD8+ T cells was analyzed by Image Pro-Plus software (Media Cybernetics, Silver Spring, MD, USA).

### Statistical Analysis

GraphPad 6 software (San Diego, CA, USA) was used for all data analyses. The difference between two independent datasets was analyzed by Student's t test. The difference in survival time was analyzed by the Kaplan-Meier method and a log rank test. Data are presented as mean ± SD, and $p < 0.05$ was considered significant for all tests.

## SUPPLEMENTAL INFORMATION

Supplemental Information can be found online at https://doi.org/10.1016/j.omto.2019.06.002.

## AUTHOR CONTRIBUTIONS

Z.L. developed the experiments, carried out the parameter estimations, and wrote the main part of the manuscript. Y.Z., H.C., and F.Z. took part in development of the mouse model. L.D. wrote parts of the manuscript and reviewed the manuscript. R.L. participated in coordination of the study and reviewed the manuscript. All authors read and approved the final manuscript.

## CONFLICTS OF INTEREST

L.D. is an employee of Shanghai HyCharm Inc. A patent was filed for the methods of the immunogen design (application number WO2014/183649A1). This does not alter the author's adherence to all journal policies regarding sharing of data and materials.

## ACKNOWLEDGMENTS

This work was supported by the National Key Research and Development Program of China (2017YFC0909002) and the National Science and Technology Major Projects of China (Major Infectious Diseases 2017ZX10201301-003-004).

## REFERENCES

1. Greenwald, R.J., Freeman, G.J., and Sharpe, A.H. (2005). The B7 family revisited. Annu. Rev. Immunol. *23*, 515–548.
2. Blank, C., Gajewski, T.F., and Mackensen, A. (2005). Interaction of PD-L1 on tumor cells with PD-1 on tumor-specific T cells as a mechanism of immune evasion: implications for tumor immunotherapy. Cancer Immunol. Immunother. *54*, 307–314.
3. Zhou, Q., Munger, M.E., Veenstra, R.G., Weigel, B.J., Hirashima, M., Munn, D.H., Murphy, W.J., Azuma, M., Anderson, A.C., Kuchroo, V.K., and Blazar, B.R. (2011). Coexpression of Tim-3 and PD-1 identifies a CD8+ T-cell exhaustion phenotype in mice with disseminated acute myelogenous leukemia. Blood *117*, 4501–4510.
4. Sharpe, A.H., Wherry, E.J., Ahmed, R., and Freeman, G.J. (2007). The function of programmed cell death 1 and its ligands in regulating autoimmunity and infection. Nat. Immunol. *8*, 239–245.
5. Muenst, S., Schaerli, A.R., Gao, F., Däster, S., Trella, E., Droeser, R.A., Muraro, M.G., Zajac, P., Zanetti, R., Gillanders, W.E., et al. (2014). Expression of programmed death ligand 1 (PD-L1) is associated with poor prognosis in human breast cancer. Breast Cancer Res. Treat. *146*, 15–24.
6. Frigola, X., Inman, B.A., Lohse, C.M., Krco, C.J., Cheville, J.C., Thompson, R.H., Leibovich, B., Blute, M.L., Dong, H., and Kwon, E.D. (2011). Identification of a soluble form of B7-H1 that retains immunosuppressive activity and is associated with aggressive renal cell carcinoma. Clin. Cancer Res. *17*, 1915–1923.
7. Kang, M.J., Kim, K.M., Bae, J.S., Park, H.S., Lee, H., Chung, M.J., Moon, W.S., Lee, D.G., and Jang, K.Y. (2013). Tumor-infiltrating PD1-Positive Lymphocytes and FoxP3-Positive Regulatory T Cells Predict Distant Metastatic Relapse and Survival of Clear Cell Renal Cell Carcinoma. Transl. Oncol. *6*, 282–289.
8. Zhang, J., Gao, J., Li, Y., Nie, J., Dai, L., Hu, W., Chen, X., Han, J., Ma, X., Tian, G., et al. (2015). Circulating PD-L1 in NSCLC patients and the correlation between the level of PD-L1 expression and the clinical characteristics. Thorac. Cancer *6*, 534–538.
9. Spranger, S., Spaapen, R.M., Zha, Y., Williams, J., Meng, Y., Ha, T.T., and Gajewski, T.F. (2013). Up-regulation of PD-L1, IDO, and Tregs in the melanoma tumor microenvironment is driven by CD8+ T cells. Sci. Transl. Med. *5*, 200ra116.
10. Chen, L., Deng, H., Lu, M., Xu, B., Wang, Q., Jiang, J., and Wu, C. (2014). B7-H1 expression associates with tumor invasion and predicts patient's survival in human esophageal cancer. Int. J. Clin. Exp. Pathol. *7*, 6015–6023.
11. Rossille, D., Gressier, M., Damotte, D., Maucort-Boulch, D., Pangault, C., Semana, G., Le Gouill, S., Haioun, C., Tarte, K., Lamy, T., et al.; Groupe Ouest-Est des Leucémies et Autres Maladies du Sang; Groupe Ouest-Est des Leucémies et Autres Maladies du Sang (2014). High level of soluble programmed cell death ligand 1 in blood impacts overall survival in aggressive diffuse large B-Cell lymphoma: results from a French multicenter clinical trial. Leukemia *28*, 2367–2375.
12. Maute, R.L., Gordon, S.R., Mayer, A.T., McCracken, M.N., Natarajan, A., Ring, N.G., Kimura, R., Tsai, J.M., Manglik, A., Kruse, A.C., et al. (2015). Engineering high-affinity PD-1 variants for optimized immunotherapy and immuno-PET imaging. Proc. Natl. Acad. Sci. USA *112*, E6506–E6514.
13. González-Cao, M., Karachaliou, N., Viteri, S., Morales-Espinosa, D., Teixidó, C., Sánchez Ruiz, J., Molina-Vila, M.Á., Santarpia, M., and Rosell, R. (2015). Targeting PD-1/PD-L1 in lung cancer: current perspectives. Lung Cancer (Auckl.) *6*, 55–70.
14. Ott, P.A., Hodi, F.S., and Robert, C. (2013). CTLA-4 and PD-1/PD-L1 blockade: new immunotherapeutic modalities with durable clinical benefit in melanoma patients. Clin. Cancer Res. *19*, 5300–5309.
15. Chen, L., and Han, X. (2015). Anti-PD-1/PD-L1 therapy of human cancer: past, present, and future. J. Clin. Invest. *125*, 3384–3391.

16. Ceeraz, S., Nowak, E.C., and Noelle, R.J. (2013). B7 family checkpoint regulators in immune regulation and disease. Trends Immunol. *34*, 556–563.

17. Mahoney, K.M., and Atkins, M.B. (2014). Prognostic and predictive markers for the new immunotherapies. Oncology (Williston Park) *28* (*Suppl 3*), 39–48.

18. Lázár-Molnár, E., Yan, Q., Cao, E., Ramagopal, U., Nathenson, S.G., and Almo, S.C. (2008). Crystal structure of the complex between programmed death-1 (PD-1) and its ligand PD-L2. Proc. Natl. Acad. Sci. USA *105*, 10483–10488.

19. Zhang, F., Wei, H., Wang, X., Bai, Y., Wang, P., Wu, J., Jiang, X., Wang, Y., Cai, H., Xu, T., and Zhou, A. (2017). Structural basis of a novel PD-L1 nanobody for immune checkpoint blockade. Cell Discov. *3*, 17004.

20. Zhong, C., Zhang, L., Chen, L., Deng, L., and Li, R. (2017). Coagulation factor XI vaccination: an alternative strategy to prevent thrombosis. J. Thromb. Haemost. *15*, 122–130.

21. Xu, A., Zhang, L., Chen, Y., Lin, Z., and Li, R. (2017). Immunogenicity and efficacy of a rationally designed vaccine against vascular endothelial growth factor in mouse solid tumor models. Cancer Immunol. Immunother. *66*, 181–192.

22. Curran, M.A., Montalvo, W., Yagita, H., and Allison, J.P. (2010). PD-1 and CTLA-4 combination blockade expands infiltrating T cells and reduces regulatory T and myeloid cells within B16 melanoma tumors. Proc. Natl. Acad. Sci. USA *107*, 4275–4280.

23. Duraiswamy, J., Kaluza, K.M., Freeman, G.J., and Coukos, G. (2013). Dual blockade of PD-1 and CTLA-4 combined with tumor vaccine effectively restores T-cell rejection function in tumors. Cancer Res. *73*, 3591–3603.

24. Pauken, K.E., and Wherry, E.J. (2015). Overcoming T cell exhaustion in infection and cancer. Trends Immunol. *36*, 265–276.

25. Ahmad, S.M., Svane, I.M., and Andersen, M.H. (2014). The stimulation of PD-L1-specific cytotoxic T lymphocytes can both directly and indirectly enhance antileukemic immunity. Blood Cancer J. *4*, e230.

26. Munir, S., Andersen, G.H., Woetmann, A., Ødum, N., Becker, J.C., and Andersen, M.H. (2013). Cutaneous T cell lymphoma cells are targets for immune checkpoint ligand PD-L1-specific, cytotoxic T cells. Leukemia *27*, 2251–2253.

27. Gabrilovich, D.I., Ostrand-Rosenberg, S., and Bronte, V. (2012). Coordinated regulation of myeloid cells by tumours. Nat. Rev. Immunol. *12*, 253–268.

28. Weide, B., Martens, A., Zelba, H., Stutz, C., Derhovanessian, E., Di Giacomo, A.M., Maio, M., Sucker, A., Schilling, B., Schadendorf, D., et al. (2014). Myeloid-derived suppressor cells predict survival of patients with advanced melanoma: comparison with regulatory T cells and NY-ESO-1- or melan-A-specific T cells. Clin. Cancer Res. *20*, 1601–1609.

29. Woo, S.R., Turnis, M.E., Goldberg, M.V., Bankoti, J., Selby, M., Nirschl, C.J., Bettini, M.L., Gravano, D.M., Vogel, P., Liu, C.L., et al. (2012). Immune inhibitory molecules LAG-3 and PD-1 synergistically regulate T-cell function to promote tumoral immune escape. Cancer Res. *72*, 917–927.

30. Wierz, M., Pierson, S., Guyonnet, L., Viry, E., Lequeux, A., Oudin, A., Niclou, S.P., Ollert, M., Berchem, G., Janji, B., et al. (2018). Dual PD1/LAG3 immune checkpoint blockade limits tumor development in a murine model of chronic lymphocytic leukemia. Blood *131*, 1617–1621.

31. Ostuni, R., Kratochvill, F., Murray, P.J., and Natoli, G. (2015). Macrophages and cancer: from mechanisms to therapeutic implications. Trends Immunol. *36*, 229–239.

32. Gardner, A., and Ruffell, B. (2016). Dendritic Cells and Cancer Immunity. Trends Immunol. *37*, 855–865.

33. Yu, J.W., Bhattacharya, S., Yanamandra, N., Kilian, D., Shi, H., Yadavilli, S., Katlinskaya, Y., Kaczynski, H., Conner, M., Benson, W., et al. (2018). Tumor-immune profiling of murine syngeneic tumor models as a framework to guide mechanistic studies and predict therapy response in distinct tumor microenvironments. PLoS ONE *13*, e0206223.

34. Son, C.H., Bae, J.H., Shin, D.Y., Lee, H.R., Choi, Y.J., Jo, W.S., Ho Jung, M., Kang, C.D., Yang, K., and Park, Y.S. (2014). CTLA-4 blockade enhances antitumor immunity of intratumoral injection of immature dendritic cells into irradiated tumor in a mouse colon cancer model. J. Immunother. *37*, 1–7.

35. Coffelt, S.B., and de Visser, K.E. (2016). Revving Up Dendritic Cells while Braking PD-L1 to Jump-Start the Cancer-Immunity Cycle Motor. Immunity *44*, 722–724.

36. Mediavilla-Varela, M., Page, M.M., Kreahling, J., Antonia, S.J., and Altiok, S. (2017). Anti-PD1 treatment to induce M1 polarization of tumor infiltrating macrophages in a 3D ex vivo system of lung cancer patients. J. Clin. Oncol. *35*, e23090.

37. Schildberg, F.A., Klein, S.R., Freeman, G.J., and Sharpe, A.H. (2016). Coinhibitory Pathways in the B7-CD28 Ligand-Receptor Family. Immunity *44*, 955–972.

38. Holmström, M.O., Riley, C.H., Skov, V., Svane, I.M., Hasselbalch, H.C., and Andersen, M.H. (2018). Spontaneous T-cell responses against the immune check point programmed-death-ligand 1 (PD-L1) in patients with chronic myeloproliferative neoplasms correlate with disease stage and clinical response. OncoImmunology *7*, e1433521.

39. Klausen, U., Holmberg, S., Holmström, M.O., Jørgensen, N.G.D., Grauslund, J.H., Svane, I.M., and Andersen, M.H. (2018). Novel Strategies for Peptide-Based Vaccines in Hematological Malignancies. Front. Immunol. *9*, 2264.

40. DeSantis, C.E., Lin, C.C., Mariotto, A.B., Siegel, R.L., Stein, K.D., Kramer, J.L., Alteri, R., Robbins, A.S., and Jemal, A. (2014). Cancer treatment and survivorship statistics, 2014. CA Cancer J. Clin. *64*, 252–271.

41. Miller, K.D., Siegel, R.L., Lin, C.C., Mariotto, A.B., Kramer, J.L., Rowland, J.H., Stein, K.D., Alteri, R., and Jemal, A. (2016). Cancer treatment and survivorship statistics, 2016. CA Cancer J. Clin. *66*, 271–289.

42. Dagogo-Jack, I., and Shaw, A.T. (2018). Tumour heterogeneity and resistance to cancer therapies. Nat. Rev. Clin. Oncol. *15*, 81–94.

43. Chodon, T., Koya, R.C., and Odunsi, K. (2015). Active Immunotherapy of Cancer. Immunol. Invest. *44*, 817–836.

44. Fu, J., Malm, I.-J., Kadayakkara, D.K., Levitsky, H., Pardoll, D., and Kim, Y.J. (2014). Preclinical evidence that PD1 blockade cooperates with cancer vaccine TEGVAX to elicit regression of established tumors. Cancer Res. *74*, 4042–4052.

45. Chen, C.Y., Hutzen, B., Wedekind, M.F., and Cripe, T.P. (2018). Oncolytic virus and PD-1/PD-L1 blockade combination therapy. Oncolytic Virother. *7*, 65–77.

46. Rojas, J.J., Sampath, P., Hou, W., and Thorne, S.H. (2015). Defining Effective Combinations of Immune Checkpoint Blockade and Oncolytic Virotherapy. Clin. Cancer Res. *21*, 5543–5551.

47. Chong, E.A., Melenhorst, J.J., Lacey, S.F., Ambrose, D.E., Gonzalez, V., Levine, B.L., June, C.H., and Schuster, S.J. (2017). PD-1 blockade modulates chimeric antigen receptor (CAR)-modified T cells: refueling the CAR. Blood *129*, 1039–1041.

48. Serganova, I., Moroz, E., Cohen, I., Moroz, M., Mane, M., Zurita, J., Shenker, L., Ponomarev, V., and Blasberg, R. (2016). Enhancement of PSMA-Directed CAR Adoptive Immunotherapy by PD-1/PD-L1 Blockade. Mol. Ther. Oncolytics *4*, 41–54.

49. Xu, D., Jaroszewski, L., Li, Z., and Godzik, A. (2014). AIDA: ab initio domain assembly server. Nucleic Acids Res. *42*, W308-13.

50. Mittal, D., Young, A., Stannard, K., Yong, M., Teng, M.W., Allard, B., Stagg, J., and Smyth, M.J. (2014). Antimetastatic effects of blocking PD-1 and the adenosine A2A receptor. Cancer Res. *74*, 3652–3658.

51. Faustino-Rocha, A., Oliveira, P.A., Pinho-Oliveira, J., Teixeira-Guedes, C., Soares-Maia, R., da Costa, R.G., Colaço, B., Pires, M.J., Colaço, J., Ferreira, R., and Ginja, M. (2013). Estimation of rat mammary tumor volume using caliper and ultrasonography measurements. Lab Anim. (NY) *42*, 217–224.

52. Dezfouli, S., Hatzinisiriou, I., and Ralph, S.J. (2003). Enhancing CTL responses to melanoma cell vaccines in vivo: synergistic increases obtained using IFNgamma primed and IFNbeta treated B7-1+ B16-F10 melanoma cells. Immunol. Cell Biol. *81*, 459–471.

**OMTO, Volume *14***

## Supplemental Information

# A PD-L1-Based Cancer Vaccine Elicits Antitumor Immunity in a Mouse Melanoma Model

**Zhibing Lin, Yan Zhang, Huaman Cai, Fuqiang Zhou, Hongjun Gao, Li Deng, and Rongxiu Li**

## Supplemental Information

## Supplemental Figures and Legends

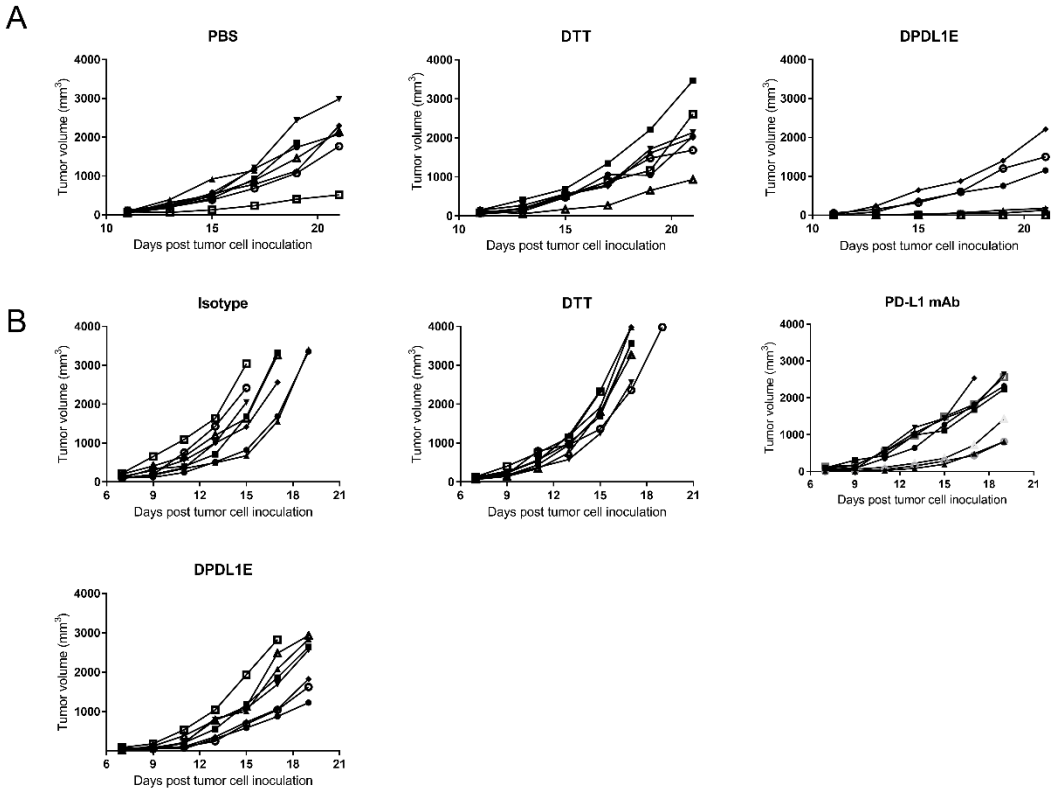


**Figure S1. Tumor growth curves of mice in preventive and therapeutic model**

(A) Tumor growth curve of individual mouse in preventive model. (B) Tumor growth curve of individual mouse in therapeutic model.

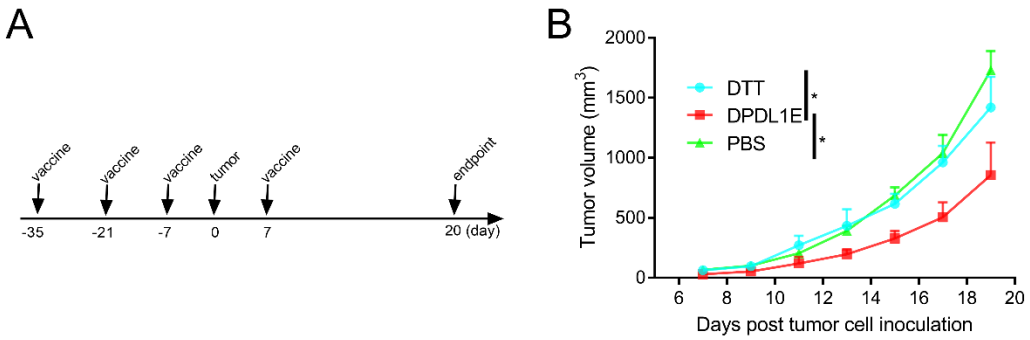


**Figure S2. DPDL1 inhibited tumor growth in CT26 colon cancer mouse model**

(A) The vaccination and tumor challenge schedule. (B) The tumor growth curve. Statistically significant differences were determined using log-rank test. * indicates $P < 0.05$

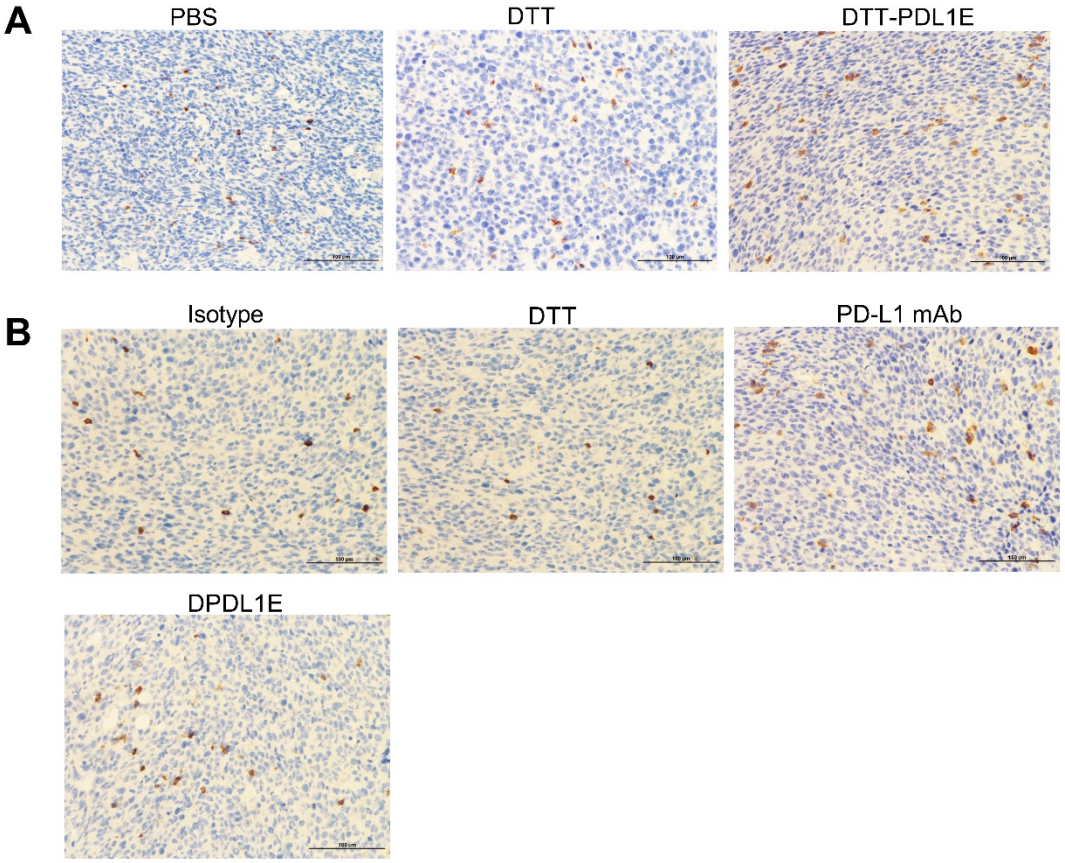


**Figure S3. DPDL1E vaccination increased CD8+ T cell infiltration in tumors.**

(A) Tumor tissues were isolated from mice in the preventive model and stained with anti-CD8α antibody. (B) Tumor tissues were isolated from mice in the therapeutic model and stained with anti-CD8α antibody.

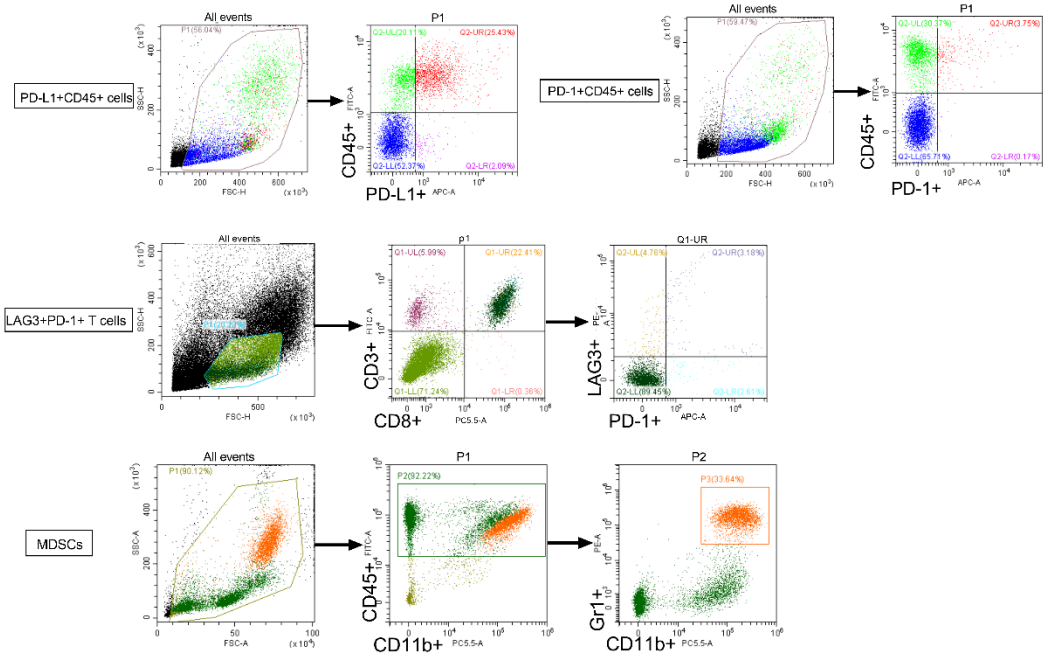


**Figure S4. The gating strategy for the frequency analyses of PD-L1+CD45+, PD-1+CD45+, LAG3+PD-1+ and MDSCs.**

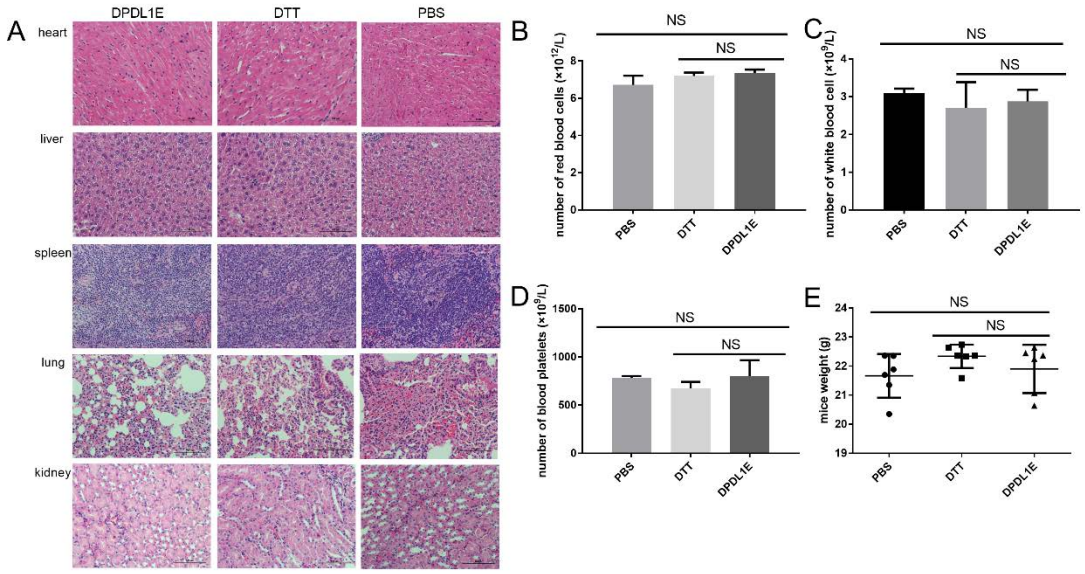


**Figure S5. The safety evaluation of DTT-PDL1E vaccine.**

(A) Mice were immunized with DTT-PDL1E, DTT or PBS three times at 2-week interval. 90 days after the third immunization, the tissue samples of heart, liver, spleen, lung, and kidney were stained with H&E. PBMC were analyzed using Auto Hematology Analyzer. The counts of red blood cells (B), white blood cells (C) and blood platelets (D) were determined. (E) The body weights of mice were measured, and the statistic difference between groups were determined by Student's *t*-test. NS stands for not significant.

**Supplemental Tables**

Table S1: The primers for mouse PD-L1 ORF amplification

| Name | Length (bp) | Tm (℃) | Sequence (5'→3') |
|---|---|---|---|
| M-PDL1-P1 | 22 | 59 | CAGTCTCCTCGCCTGCAGATAG |
| M-PDL1-P2 | 21 | 58.5 | GTGCAAGGACCAGCTGCTAAG |
| M-PDL1-P3 | 23 | 59.1 | GTCTCCTCGCCTGCAGATAGTTC |
| M-PDL1-P4 | 22 | 58.5 | CAAGCTGCCAATCGACGATCAG |

Table S2: The primers for DPDL1E amplication

| Name | Length (bp) | Tm ( ℃ | Sequence (5'→3') |
|---|---|---|---|
| DPDL1E-P1 | 27 | 57.6 | CCGAATTCCTTGATTGGGATG |
| DPDL1E-P2 | 38 | 68 | CTTTGGAGCCGTGATAGTAAACGAACCACCA CCACCCG |
| DPDL1E-P3 | 38 | 68 | CGGGTGGTGGTGGTTCGTTTACTATCACGGCT CCAAAG |
| DPDL1E-P4 | 29 | 65.1 | GGCTCGAGTTACAGTTCTGGGATGATCAGCTC |